https://dx.doi.org/10.1016/j.tws.2023.110801

Numerical investigation and design recommendation for thin-walled octagonal concrete filled steel tubes

Jiongyi Zhu[1], Junbo Chen[2], Lei Zhang[1] Yongping Zhang[1*] and Tak-Ming Chan[3]

[1] *Department of Civil Engineering, School of Mechanics and Engineering Science, Shanghai University, Shanghai, China*

[2]*School of Civil and Hydraulic Engineering, Huazhong University of Science and Technology, Wuhan, Hubei, China*

[3]*Department of Civil and Environmental Engineering, The Hong Kong Polytechnic University, Hung Hom, Hong Kong*

* Corresponding author: zhangyongping@shu.edu.cn

Abstract: With the growing applications of high strength steel in modern constructions, thin-walled steel tubes attract many attentions. Local buckling failure is the most typical failure mode in a thin-walled steel tube, and concrete filled steel tubes (CFSTs) are excellent composite members in which the occurrence of local buckling is mitigated by the infilled concrete. This paper aims to investigate the compressive strength of concrete filled thin-walled octagonal steel tubes, which have the advantages of confinement efficiency over rectangular CFSTs, and constructability over circular CFSTs. Finite element models are established and validated by the experimental results from existing literatures. A parametric study is subsequently conducted and the result shows that the buckling strength of octagonal tube is significantly improved by the infilled concrete and the enhancement percentage increases with the increase of section slenderness coefficient, and the local buckling behaviour has a minor influence to the effect of confinement. In addition, a database consisting of 37 experimental specimens and 37 FE models are developed and used to assess the design methods in current codes of practice. It is found that the design methods from ANSI/AISC 360-16 and GB 50936-2014 underestimate the load capacity of octagonal CFSTs while the design formula

from EN 1994-1-1 which considers the effect of confinement overestimates the capacity. Finally, a design model considering the buckling strength of octagonal steel tube, the influence of infilled concrete core and the effect of confinement is proposed and this model can well capture the compressive strength of octagonal CFSTs.

Keywords: Thin-walled CFSTs; Octagonal sections; Local buckling; Confinement; Design model.

1. Introduction

1.1 Research background

Concrete filled steel tubes (CFSTs) have proved to be excellent compressive structural members. The compressive strength can be enhanced from the effect of confinement. The cross-section shape significantly dominates the effectiveness of confinement in CFST. The effectiveness of confinement in circular CFSTs is much better than rectangular CFSTs[1-3], however, the rectangular section has advantages in constructability, in which the flat sides allow diverse beam-column connection types such as bolted connections and end plate connections. Recently, polygonal sections especially octagonal section have attracted many academic attentions as the section combines the merits of circular and rectangular sections, having considerable confinement effectiveness and flat sides for construction as well. The first experimental study on CFST with octagonal section was conducted in 1977 by Tomii[4], 148 CFSTs with circular, square and octagonal sections were tested and it was found that the strength enhancement from confinement in octagonal CFST is higher than square counterparts, but lower than that in circular CFSTs. From then on, a series of experimental investigations were conducted on octagonal CFSTs[3, 5-11]. Among them, Ding[7] tested eight octagonal CFSTs with compact sections, and based on their test results, a design formula of load bearing capacity was proposed. Zhu and Chan[10] tested 21 CFST specimens with circular, square and octagonal section and conducted a systematic comparison of the effectiveness of confinement between CFSTs with these three different cross-section shapes and proposed a confinement coefficient for

58 octagonal CFSTs. Fang et al.[8] conducted an experimental study on octagonal CFSTs
59 with high strength steel tube, the yield strength of the external steel tube is 760 MPa
60 and concrete cylinder strength ranges from 56.8 MPa to 89.6 MPa. Compressive
61 behaviour of octagonal CFSTs with slender sections were also investigated[9, 12, 13].
62 Lim et al.[9] tested eight irregular octagonal CFSTs with thin-walled steel tubes, the
63 width to thickness ratio ranges from 65 to 89, and in the tests, elastic local buckling was
64 found in those octagonal CFSTs with large *D/t* ratio. Recently, Chen and Chan[12]
65 tested 20 octagonal CFSTs which include both compact and slender sections, and the
66 design methods in current design codes including EN 1994-1-1[14] and ANSI/AISC
67 360-16[15] were evaluated. It was found that the Eurocode overestimates the load
68 capacity of octagonal CFSTs with slender section when confinement effect is
69 considered. The local buckling behaviour of thin-walled CFSTs has been studied. Liang
70 et al.[16] argued that the section slenderness of rectangular CFSTs affects both the
71 strength and the ductility of the CFST columns under compression. Cheng et al.[17]
72 tested nine square CFSTs and found that the buckling behaviour of steel tube also
73 affects the confinement to the concrete core. Numerical investigations such as finite
74 element analysis on thin-walled octagonal CFSTs were also conducted[13]. However,
75 the elastic local buckling strength of thin-walled octagonal steel tubes in CFSTs has not
76 been fully investigated and the current design formulas have not considered the
77 reduction of the strength in slender steel tubes. Generally, the steel ratio in thin-walled
78 CFSTs with normal grade steel is low leadsh lead to the strength reduction in the steel
79 tube from local buckling have minon influence to the load capacity of the composite

section, however, when the high strength steel tube is adopted, the steel ratio increases and the strength reduction should be considered. Thus, to well capture the load capacity of thin-walled octagonal CFSTs, the local buckling behaviour of octagonal steel tube with infilled concrete should be understood.

The local buckling behaviour of octagonal hollow steel tubes has been investigated by many researchers. Cold-formed and welded octagonal hollow steel tubes were experimentally and numerically studied, and many prediction models of the buckling strength of octahollowollows steel tube were proposed[18-24]. Zhu and Chan[23] indicated the current cross-section slenderness limits in EN 1993-1-1[25] and ASCE/SEI 48-11[26] for rectangular section are not applicable for the octagonal section and a new limit was proposed. Fang et al.[20, 27] extended the studies of octagonal hollow steel tubes from normal strength steel to high strength steel with steel grade S690, and three types of section with different fabrication routines were considered including one welded section and two cold-formed sections. Recently, Chen et al.[24]proposed a design method for the octagonal hollow steel tubes with both normal strength and high strength steel, and it was indicated that in the design of cold-formed octagonal sections, the influence of the strength enhancement at corner region from the press-braking process should be considered in the calculation of cross-section capacity as the total corner area in the octagonal section is non-negligible. The existing research can well capture the cross-section slenderness limit and buckling strength of octagonal hollow steel tube, however, in CFSTs, the infilled concrete prevents the inward local buckling of steel tubes and influences the buckling behaviour. Thus, for thin-walled

102 octagonal CFSTs, the effect of infilled concrete core to the buckling behaviour of the
103 steel tube should be studied.

104 In current design provisions, the section slenderness is limited and only the design
105 formulas of circular sections and rectangular section of CFSTs are specified except
106 Chinese code GB 50936-2014[28] which considers octagonal CFSTs. Chen and
107 Chan[12] suggested the design formula of cross-sectional capacity in Chinese code GB
108 50936-2014[28] for circular section could be used for octagonal section and the
109 equivalent circumcircle method could be used in EN 1993-1-1[25] and ASCE/SEI 48-
110 11[26]. However, the design formula for the load capacity of octagonal CFSTs with
111 slender section is not specified in current design codes as well as the strength reduction
112 due to the buckling of the external steel tube.

113 This paper focuses on the compressive strength of octagonal shaped CFSTs with
114 slender cold-formed octagonal steel tube. Finite element analysis which considers the
115 effects of cold-forming process and local imperfection of steel tube was conducted and
116 validated by the experimental results. The validated FE model was then adopted to carry
117 out a parametric study. Based on the numerical results, the buckling strength of thin-
118 walled octagonal steel tubes in CFST was obtained, the influences of local buckling of
119 steel tube to the compressive behaviour of octagonal CFST were discussed, and finally
120 a new design formula was proposed for the thin-walled octagonal CFSTs. It should be
121 noted that in this paper thin-walled CFST or CFST with slender section represent a
122 CFST with steel tube having local buckling before yielding of steel.

1.2 Existing experimental database

Experimental results of octagonal CFSTs were collected from existing literatures of Chen and Chan[12], Zhu and Chan[10, 11] and Ding[7]. The database includes 37 test results of cold-formed octagonal CFST stub columns under monotonic axial compression. Detailed geometric properties and material properties are listed in Table 1, where B is nominal width of section, b is flat width which excluding the corner region, H is the inscribed diameter of the octagonal section, L is the length of the specimen, r_o and r_i are the outer radius and inner radius of corners respectively (see Figure 1), $f_c^{'}$ is the cylinder strength of the infilled concrete, f_y is the 0.2% proof strength of the steel tube at flat region, ξ confinement ratio which is defined as in Eq. 1, where A_c and A_s are the cross-sectional area of concrete core and steel tube respectively. λ_c is the coefficient of section slenderness which is defined in Eq. 2, where E is the Young's modulus of steel.

$$\xi = A_s f_y / A_c f_c^{'} \tag{1}$$

$$\lambda_c = (b/t)\sqrt{f_y / E} \tag{2}$$

The current test database covers a range of b/t ratio from 11 to 52, both normal and high strength concrete whose cylinder strength ranges from 28 MPa to 101 MPa, and a range of steel grade with 0.2% proof strength from 311 MPa to 581 MPa. In Table 1, it could be found the section slenderness coefficients λ_c of the test specimens are mostly smaller than 1.4. In European standard EN 1994-1-1[14], the slenderness limit for CFSTs with rectangular sections is $b/t \leq 52\sqrt{235/f_y}$, which is equivalent to the limit of $\lambda_c \leq 1.75$,. According to this limit, only a few test specimens in the database are with

slender cross-sections. However, previous studies on octagonal hollow steel sections indicated that the limit should be relaxed due to the octagonal cross-section shape[20, 23, 24]. A well validated numerical model should be generated to extend the current database to cover more data of octagonal CFSTs with slender section, and the numerical results allow to further investigati the buckling behaviour of the thin-walled octagonal steel tube.

Table 1. Collected database of octagonal CFSTs

Reference	Specimens	B (mm)	b (mm)	L (mm)	t (mm)	r_o (mm)	r_i (mm)	f_y (MPa)	f_c' (MPa)	ξ	λ_c	N (kN)
Chen and Chan[12]	O60-3–30	61	55	433	3.1	7	3.5	547	32	1.79	0.92	1616
	O60-3–50	61	56	431	3.0	6.5	3.5	547	55	1.09	0.93	2053
	O60-3–50#	61	55	432	3.1	7	3.5	547	55	1.11	0.92	1982
	O60-3–90	61	55	432	3.0	7	3.5	547	92	0.66	0.93	2565
	O75-3–30	77	71	539	3.1	7	4	547	28	1.62	1.18	2033
	O75-3–50	76	71	540	3.1	7	4	547	55	0.87	1.18	2903
	O75-3–90	76	71	543	3.0	7	3.5	547	92	0.52	1.18	3702
	O75-3–90#	76	70	543	3.0	7	3.5	547	92	0.53	1.18	3753
	O75-6–30	78	68	544	5.9	11	5	581	28	3.40	0.61	3550
	O75-6–50	78	68	544	5.9	11	5	581	55	1.82	0.61	4211
	O75-6–90	77	68	543	5.8	11	5	581	92	1.09	0.62	5098
	O75-6–90#	77	68	543	5.8	11	5	581	92	1.10	0.62	5033
	O90-3–30	92	85	646	3.0	7.5	4	547	28	1.35	1.43	2532
	O90-3–50	91	86	647	3.1	7	3.5	547	55	0.72	1.43	3695
	O90-3–90	91	85	648	3.1	7	3.5	547	92	0.44	1.43	4891
	O90-3–90#	91	86	649	3.1	7	3.5	547	92	0.44	1.43	5116
	O105-3–30	107	101	755	3.0	7	4	547	32	0.98	1.70	3527
	O105-3–30#	106	101	753	3.0	7	4	547	32	0.99	1.69	3538
	O105-3–50	106	101	756	3.0	7	3.5	547	55	0.62	1.69	4641
	O105-3–90	106	101	759	3.0	7	3.5	547	92	0.37	1.69	6317
Zhu and Chan[10]	40O1-1	74	60	695	5.6	16.7	11.1	384	38	1.71	0.56	2733
	40O1-2	74	60	695	5.6	16.7	11.1	384	38	1.71	0.56	2680
	60O1-1	74	60	695	5.6	16.7	11.1	384	72	0.93	0.56	3543
	60O1-2	74	60	695	5.6	16.7	11.1	384	72	0.93	0.56	3549
	80O1-1	74	60	695	5.6	16.7	11.1	384	101	0.67	0.56	4199
	80O1-2	74	60	695	5.6	16.7	11.1	384	101	0.67	0.56	4153
	80O1-3	74	60	695	5.6	16.7	11.1	384	101	0.67	0.56	4203
Zhu and Chan[11]	O-CF-1	60	52	450	2.9	9.3	6.2	296	100	0.32	0.77	1970
	O-CF-2	60	52	450	2.9	9.3	6.2	296	100	0.32	0.77	2024
Ding et al.[7]	OST1-A	201	201	1500	3.9	-	-	311	32	0.38	2.01	9297
	OST1-B	199	199	1500	4.0	-	-	311	32	0.40	1.92	9311
	OST2-A	200	200	1500	6.0	-	-	321	32	0.62	1.30	10502
	OST2-B	197	197	1500	5.9	-	-	321	32	0.62	1.31	10713
	OST3-A	200	200	1500	3.9	-	-	311	46	0.28	1.96	12362
	OST3-B	199	199	1500	4.0	-	-	311	46	0.29	1.91	12357
	OST4-A	197	197	1500	5.9	-	-	321	46	0.45	1.31	12992
	OST4-B	198	198	1500	6.0	-	-	321	46	0.45	1.29	13263

# indicates repeated specimen

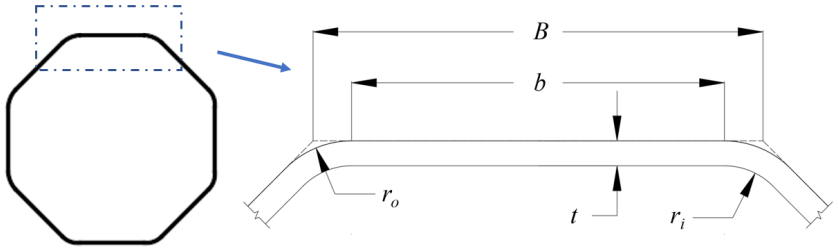

Figure 1. Geometrical information and definition of symbols of octagonal section

2. Numerical investigations

To extend current database of slender octagonal CFSTs, finite element analysis was conducted via the commercial software package ABAQUS[29], the following sections demonstrated the details of established finite element model, and the validation of the model against the experimental data of both compact and slender octagonal CFST specimens is presented. Based on the well validated model, parametric study was conducted to exam the influence of different parameters to the buckling strength of steel tube and to generate more data covering wider ranges of parameters.

2.1 Finite element models

2.1.1 Modeling of steel tube

In the finite element models, four-node shell element (S4R in ABAQUS) was selected for the external steel tube which have been widely adopted and validated by the existing literatures[8, 23]. In the validation of the FE models, the measured geometric and material properties reported in the literature were used to replicate the test results, and in the parametric studies, the cold-formed steel tube were considered. An outer corner radius of $3t$ and inner corner radius of $2t$ were used for the cold-formed corners. The material properties of flat and corner regions are both considered. The

cold-forming process enhances the yield strength at corner due to the strain hardening. As the corner region of the specimens in the database accounts for up to 30% of the cross-sectional gross area, the strength enhancement in corner region was considered. In validation, the stress-strain relationships of steel at flat and corner regions are used if the coupon test results are reported in details, otherwise, a three-stage nonlinear model from Chen et al.[30] was adopted, which was proposed on the basis of a large amount of coupon test data. To precisely capture the buckling strength and failure mode of the steel tube, in ABAQUS, the *imperfection option was used to replicate the imperfection profile. The lowest elastic buckling mode from elastic buckling analysis of octagonal hollow steel tube was used as the imperfection profile, and an amplitude of t/10 was used[23, 24]. Residual stresses from cold-forming and welding process are not considered in the FE models due to their minor influence to the local buckling behaviour of tubular steel stub columns under uniaxial compression[23, 30].

2.1.2 Modelling of concrete

Eight-node solid elements (C3D8R) were used for the modelling of concrete core. The constitutive model of confined concrete core inside the steel tube for circular section suggested by Tao et al.[31] was adopted. The stress-strain model is a three-stage curve as shown in Figure 2. The expressions of OA, AB and BC stages are shown in Eqs. 3-10, where σ and ε are the uniaxial stress and strain of concrete, $f_c^{'}$ is the compressive cylinder strength of concrete, f_B is the confining stress at point B, f_r is the residual stress, ε_{co} and ε_{cc} are the strains at point A and point B respectively.

$$\sigma=\begin{cases}\dfrac{\sigma}{f_c^{'}}=\dfrac{A\cdot X+B\cdot X^2}{1+(A-2)X+(B+1)X^2} & 0<\varepsilon\le\varepsilon_{c0}\\ f_c^{'} & \varepsilon_{c0}<\varepsilon\le\varepsilon_{cc}\\ f_r+\left(f_c^{'}-f_r\right)\exp\left[-\left(\dfrac{\varepsilon-\varepsilon_{cc}}{\alpha}\right)^{\beta}\right] & \varepsilon\ge\varepsilon_{cc}\end{cases} \tag{3}$$

$$X=\frac{\varepsilon}{\varepsilon_{co}};\quad A=\frac{E_c\varepsilon_{co}}{f_c^{'}};\quad B=\frac{(A-1)^2}{0.55}-1 \tag{4}$$

$$\varepsilon_{co}=0.00076+\sqrt{\left(0.626f_c^{'}-4.33\right)\times10^{-7}} \tag{5}$$

$$\frac{\varepsilon_{cc}}{\varepsilon_{c0}}=e^{k},\ \ k=\left(2.9224-0.00367f_c^{'}\right)\left(\frac{f_B}{f_c^{'}}\right)^{0.3124+0.002f_c} \tag{6}$$

$$f_B=\frac{\left(1+0.027f_y\right)\cdot e^{-0.02\frac{D}{t}}}{1+1.6e^{-10}\cdot\left(f_c^{'}\right)^{4.8}} \tag{7}$$

$$f_r=0.7\left(1-e^{-1.38\xi_c}\right)f_c^{'}\le0.25f_c^{'} \tag{8}$$

$$\alpha=0.04-\frac{0.036}{1+e^{6.08\xi_c-3.49}} \tag{9}$$

$$\beta=1.2 \tag{10}$$

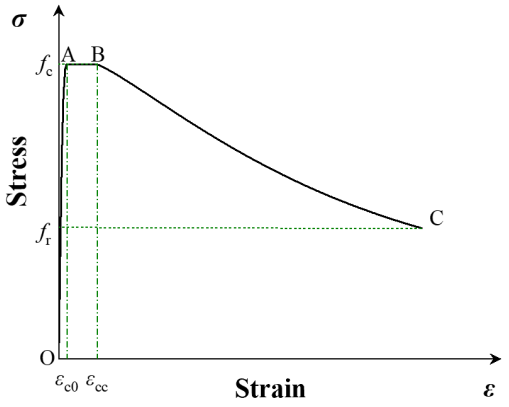

Figure 2. Constitutive model of concrete

The plastic parameters in Concrete damaged plastic (CPD) model for concrete are specified in Eqs.11-13. K_c is the ratio of the second stress invariant on the tensile meridian to that on the compressive meridian. K_c and the dilation angle φ are adopted

196 from the empirical equations proposed in Tao et al.[31]. $\frac{f_{b0}}{f_c^{'}}$ is the ratio between biaxial

197 compression and uniaxial compression concrete strength, and the equation proposed in

198 Papanikolaou and Kappos [32] was used. The flow potential eccentricity is 0.1, the

199 viscosity is 0.

$$K_c = \frac{5.5}{5+2\left(f_c^{'}\right)^{0.0075}} \tag{11}$$

$$\frac{f_{b0}}{f_c^{'}} = 1.5\left(f_c^{'}\right)^{-0.075} \tag{12}$$

$$\varphi = \begin{cases} 56.3\left(1-\xi_c\right) & \xi_c \le 0.5 \\ 6.672e\dfrac{7.4}{4.64+\xi_c} & \xi_c > 0.5 \end{cases} \tag{13}$$

200 **2.1.3 Boundary conditions and mesh convergence studies**

201 The boundary condition of the FE models is fix-fix end constraint. Each end of the

202 column was coupled with a reference point which is restrained in all degrees of freedom

203 except the loading direction in top reference point where the axial displacement was

204 applied. The interaction behaviour between concrete core and steel tube is surface to

205 surface contact and "Hard" contact which allows the separation of the two surfaces after

206 contact was used for the normal contact behaviour and Coulomb friction model was

207 used for the tangential contact behaviour. The adopted coefficient of friction between

208 concrete and steel is 0.3[11]. To achieve the balance between accuracy and computation

209 efficiency, mesh convergence study was conducted. Based on the comparison of axial

210 load to axial shortening curves, the mesh size of $B/10$ is adopted for all the FE models.

211 **2.2 Validation of FE models**

212 The experimental results of six specimens from Zhu and Chan[10], Chen and

213 Chan[12] and Ding et al.[7] were used to validate the FE models, among them the
214 specimens 30O-1 and 50O-1 from Zhu and Chan[10] are with compact section and
215 specimens O90-3-50 and O105-3-50 from Chen and Chan[12] as well as OST1-A and
216 OST3-A from Ding et al.[7] are with slender section according to the section
217 slenderness limit proposed for the octagonal hollow section[24]. Figure 3 shows the
218 comparison of axial load-shortening curves between test and FE results. It could be
219 found that the model can well capture the ultimate strength as well as the post-peak
220 softening behaviour of the specimens with compact and slender section. Figure 4 shows
221 the comparison of failure modes between experimental observation and FE results. It
222 could be found the FE model can reasonably capture the failure mode of the compact
223 and slender test specimens. Figure 5 shows the details of FE results for specimen OST1-
224 A [7]. In Figure 5a, axial stress-strain curves of the external steel tubes with and without
225 initial imperfection were presented. It could be found both the ultimate stresses are
226 smaller than the yield strength and the reduction from the model with initial
227 imperfection is lower than that without imperfection. According to the observations
228 from the failure modes, local buckling occurred in both models but the buckling
229 deformation is small in the model without imperfection. In addition, test results of two
230 hollow octagonal steel tubes from Chen et al.[19] was adopted for the validation. Figure
231 6 shows the model can well capture both the stress-strain curves and failure mode of
232 octagonal hollow steel tubes under compression. Figure 7 illustrated the predictions of
233 load bearing capacity for all the specimens in database, the mean value of N_{FE}/N_{test} is
234 0.95 and COV is 5.8%. In conclusion, the established FE models have the ability to

predict the failure mode, load capacity and axial load-shortening relationship of the octagonal CFSTs with slender section with local buckling failure.

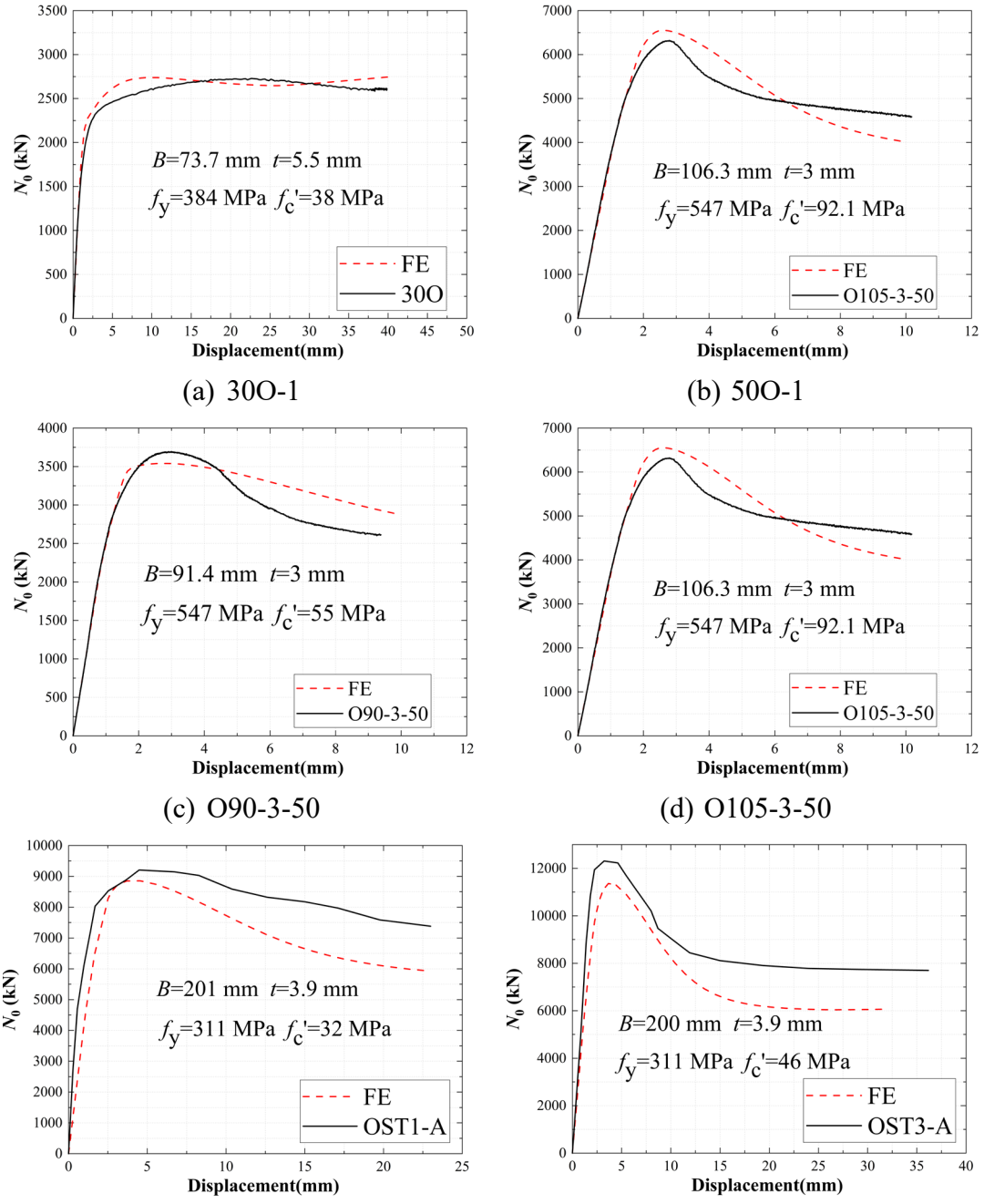

(a) 30O-1 (b) 50O-1

(c) O90-3-50 (d) O105-3-50

(e) OST1-A (f) OST3-A

Figure 3. Validation of stress-strain curves between FE and test results

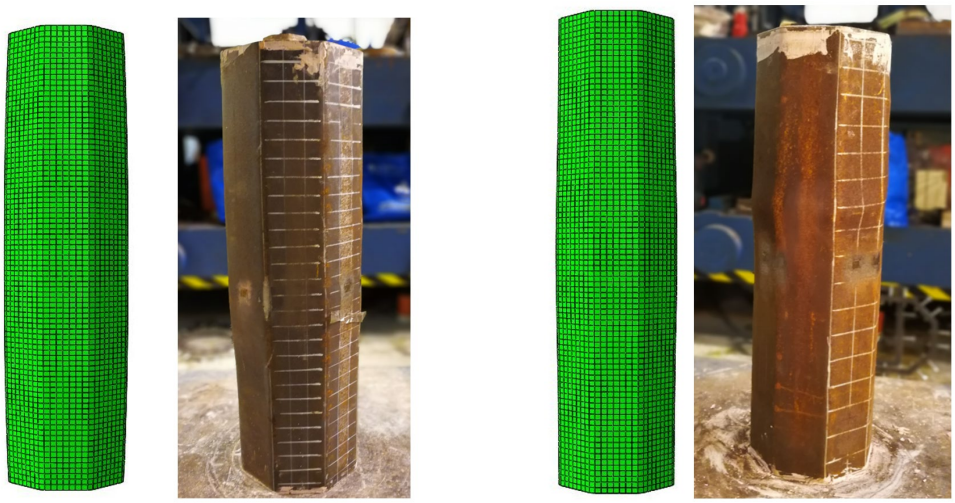

30O-1 50O-1

OST1-A OST3-A

Figure 4. Comparison of failure modes between FE and test results

238

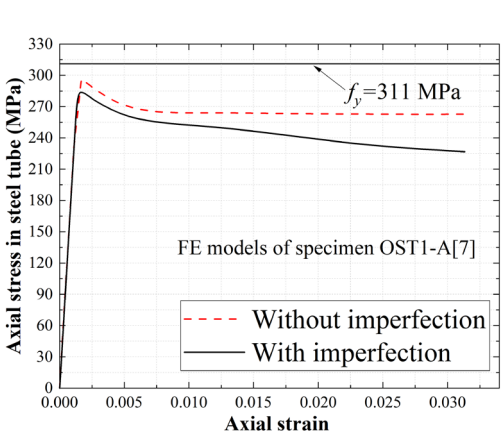

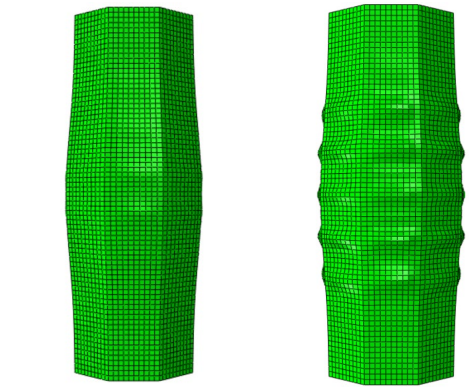

Without imperfection With imperfection (w=t/10)

(a) (b)

Figure 5. FE results of specimen OST1-A with and without imperfection: (a) Stress-strain curves of the external steel tubes; (b) Failure modes

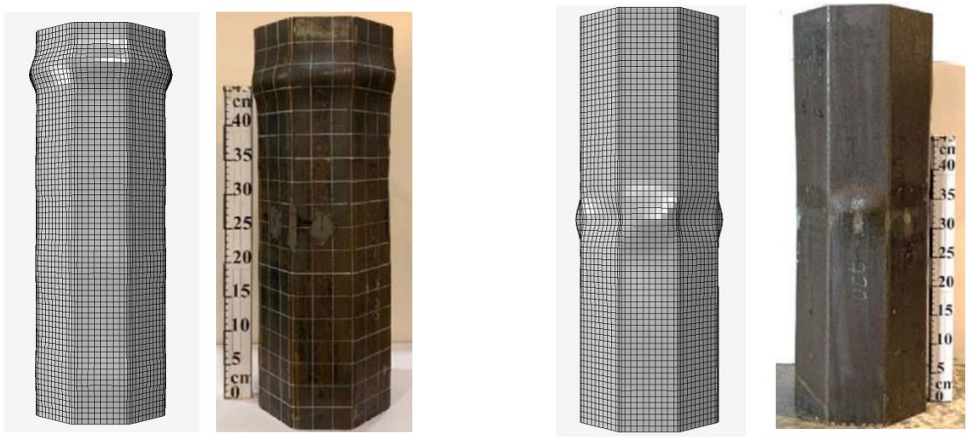

Figure 6. Validation of octagonal hollow steel tubes

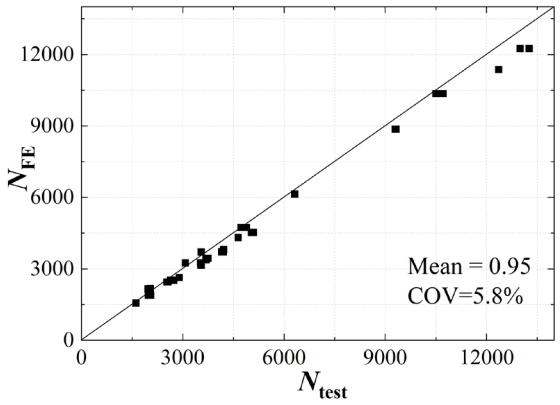

Figure 7. Prediction of load capacity from FE models

2.3 Parametric study

Based on the validated FE model, a parametric study was conducted to analyse the influence of relevant parameters to the buckling behaviour of the steel tube and generate additional data to extend the database. Totally 37 numerical models were established

and analyzed. The section slenderness coefficient λ_c ranges from 0.6 to 5.9 and most of them are slender section according to the section classification limits from Chen et al.[24] for octagonal hollow tubular section. Three steel grades (i.e S355, S460 and S690) were considered, and the yield strength and ultimate strength of the material are adopted from the Zhu and Chan[23], Fang et al.[27] and Chen et al.[30]. The effect of strain hardening at corner regions of steel tube is also considered. Three concrete strengths were adopted which are 30 MPa, 50 MPa and 80 MPa. Additionally, for each series of octagonal CFSTs with same steel section, a corresponding hollow section was also examined for comparison of local buckling strength. The details of FE models in parametric study is shown in Table 2 and the numerical results are shown in Table 3. The label system of FE models is defined as O-X-Y-Z where O indicates octagonal cross-section, X indicates thickness of steel tube, Y indicates concrete cylinder strength, Z stands for steel grades. In Table 3, N_{FE}, $N_{FE,s}$ and $N_{FE,c}$ are the axial load on whole section, steel tube and concrete core at ultimate load respectively, N_{sy} is the nominal load capacity of steel tube which is equal to $A_s f_y$, $N_{FE,h}$ is the load capacity of steel tube without concrete core. Figure 8 shows the relationship of section slenderness coefficient and the normalised strength of steel tube in octagonal CFST (i.e. $N_{FE,s}/N_{sy}$). It could be found that the strength of the steel tube in CFST is lower than its yield strength. Even for those compact sections without local buckling behaviour, there are almost 5% reductions in their strengths. The interpretation is that the lateral expansion of concrete core generates lateral stress in the steel tube which reduce the axial stress after steel is yield. Another observation is that with the increase of the section slenderness coefficient,

the normalised strength of steel tube reduces to about 80% of yield strength due to the local buckling. To precisely capture the section slenderness limit for thin-walled octagonal CFST, the failure modes of the specimens with λ_c ranges from 1.5 to 2.0 was compared, and it was observed that the local buckling failure occurred after the peak load was reached when λ_c=1.69 (see Figure 9), Thus, a new slenderness limit (λ_c=1.69) is proposed for thin-walled octagonal CFST.

Table 2. Details of parametric study

Parameters	**Details**
Element type	C3D8R (Concrete), S4R (Steel)
Mesh density	*B*/10 mm
Yield stress (MPa)	379 (Flat region) + 548 (corner region), 541+655, 762+802
Imperfection profiles	Imperfection pattern from buckling analysis
Imperfection amplitude	*t*/10
Corner radius	3*t* (outer radius)
Concrete strength (MPa)	30, 50, 80
λ_c	0.6 to 5.9

Table 3 Results of parametric study

Specimens	λ_c	N_{FE} kN	$N_{FE,s}$ kN	$N_{FE,c}$ kN	N_{AISC1} kN	N_{AISC2} kN	N_{EC4-1} kN	N_{EC4-2} kN	$N_{Z\&C}$ kN	N_{GB} kN
O-5-30-355	0.74	3582	1413	2169	2607	2740	2807	3870	3503	2947
O-4-30-355	0.96	3112	1132	1980	2338	2473	2541	3396	3101	2659
O-3-30-355	1.31	2620	844	1776	2066	2202	2272	2915	2694	2367
O-2-30-355	2.02	2164	559	1605	1791	1490	2001	2429	2281	2071
O-1-30-355	4.14	1770	271	1500	1155	1141	1726	1938	1865	1771
O-5-30-460	0.89	4489	1966	2523	3238	3371	3438	4905	4398	3721
O-4-30-460	1.14	3849	1585	2264	2846	2944	3049	4232	3823	3294
O-3-30-460	1.57	3192	1189	2004	2449	2243	2655	3549	3240	2854
O-2-30-460	2.41	2543	784	1760	2030	1619	2257	2856	2649	2402
O-1-30-460	4.95	1909	342	1568	1155	1173	1855	2154	2051	1939
O-5-30-690	1.06	5717	2760	3017	4099	3993	4299	6279	5593	4912
O-4-30-690	1.36	4807	2192	2616	3538	3527	3741	5346	4790	4280
O-3-30-690	1.86	3922	1650	2272	2971	2583	3177	4395	3974	3616
O-2-30-690	2.86	3132	1011	2121	2223	1767	2607	3428	3145	2925
O-1-30-690	5.87	2106	443	1663	1155	1209	2031	2446	2302	2208
O-5-50-355	0.74	4341	1426	2915	3361	3583	3694	4723	4367	3755
O-4-50-355	0.96	3866	1140	2726	3105	3331	3444	4268	3983	3475
O-3-50-355	1.31	3403	850	2553	2846	3074	3191	3808	3595	3188
O-2-50-355	2.02	3024	564	2460	2584	1634	2935	3344	3203	2896
O-1-50-355	4.14	2676	276	2400	1662	1662	2676	2878	2808	2598
O-5-50-460	0.89	5278	1996	3283	3992	4214	4325	5751	5257	4557
O-4-50-460	1.14	4614	1601	3013	3613	3776	3951	5098	4701	4146
O-3-50-460	1.57	3942	1192	2751	3229	2886	3573	4436	4138	3718
O-2-50-460	2.41	3360	757	2603	2812	2273	3191	3766	3567	3275
O-1-50-460	4.95	2836	359	2478	1819	1837	2805	3091	2992	2817
O-5-50-690	1.06	6499	2747	3752	4853	4675	5186	7121	6450	5659
O-4-50-690	1.36	5642	2218	3424	4305	4158	4644	6207	5665	5057

O-3-50-690	1.86	4749	1658	3091	3751	3225	4095	5278	4868	4417
O-2-50-690	2.86	3885	1054	2831	2901	2421	3541	4334	4060	3741
O-1-50-690	5.87	2956	439	2517	1819	1874	2981	3378	3241	3033
O-5-80-355	0.74	5358	1427	3931	4492	4847	5024	6010	5669	5118
O-4-80-355	0.96	4989	1146	3843	4256	4617	4797	5586	5312	4843
O-3-80-355	1.31	4637	854	3783	4017	4380	4568	5156	4952	4561
O-2-80-355	2.02	4369	566	3803	3775	3124	4335	4724	4590	4271
O-5-80-460	1.02	6273	2018	4255	5123	5478	5655	7029	6552	5857
O-4-80-460	1.27	5679	1621	4058	4763	5025	5305	6406	6024	5456
O-3-80-460	1.69	5142	1210	3932	4400	3850	4950	5776	5490	5036
O-2-80-460	2.54	4702	805	3898	3986	3253	4592	5140	4950	4597
O-5-80-690	1.20	7584	2791	4793	5984	5699	6516	8390	7739	6400
O-4-80-690	1.51	6698	2231	4467	5456	5106	5997	7506	6982	5775
O-3-80-690	2.01	5834	1603	4230	4922	4189	5472	6609	6215	5110
O-2-80-690	3.01	5097	1001	4095	3918	3401	4942	5701	5438	4409
O-1.3-50-460	3.90	2990	468	2522	2004	1942	2921	3294	3165	2956
O-1.4-50-460	3.63	3039	504	2534	2091	1983	2960	3361	3222	3002
O-1.5-50-460	3.38	3085	541	2544	2192	2026	2998	3429	3280	3048
O-6-50-460	0.85	5936	2380	3556	4367	4585	4694	6393	5805	4949
O-6-80-690	1.00	8490	3319	5171	6506	6849	7029	9259	8484	7516
O-7-50-460	0.73	6603	2761	3842	4738	4952	5059	7025	6344	5321
O-7-80-690	0.86	9376	3834	5543	7022	7365	7536	10112	9217	7999
O-8-50-460	0.63	7292	3146	4147	5105	5315	5420	7645	6873	5670
O-8-80-690	0.75	10282	4348	5934	7532	7869	8037	10950	9937	8426

276

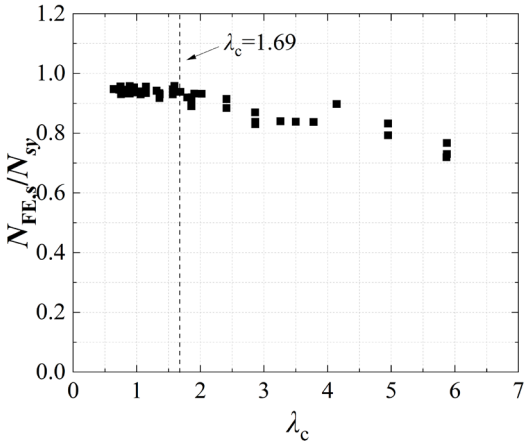

Figure 8. Reduction of strength in steel tube

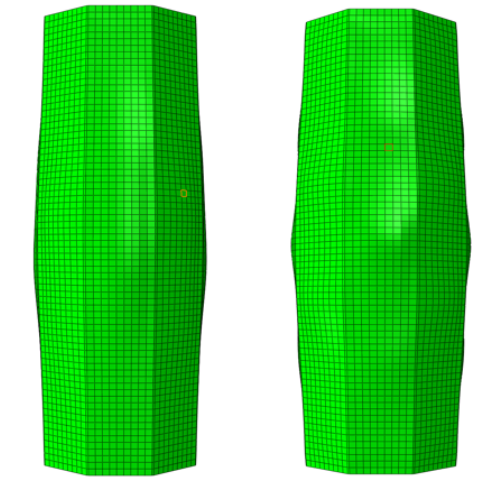

Figure 9. Comparison of failure modes of octagonal CFSTs

277 **2.3.1 Influence of infilled concrete to the buckling behaviour of steel tube**

278 Figure 8 and Figure 9 have shown that the local buckling failure occurred in the
279 octagonal steel tube in CFST and the strength of steel tube is reduced, but the influence
280 of concrete core to the buckling strength is still unclear. To investigate the influence of
281 concrete core, a companion model with hollow section was established with same

geometric properties, same material properties and same imperfection profile for each series of octagonal CFSTs. Figure 10 shows the deformation and axial stress distribution nephogram of octagonal steel tube with and without concrete core at peak load. The comparison shows the infilled concrete core significantly suppress the developing of local buckling and the strength reduction due to the buckling. The comparison between the buckling strength of steel tube with and without concrete core (i.e. $N_{FE,s}/N_{FE,h}$) is shown in Figure 11. It could be found that when the section slenderness coefficient λ_c is less than 1.2 (i.e. the slenderness limit for hollow octagonal steel tubes), the ratio of $N_{FE,s}/N_{FE,h}$ is around 0.95, and as the λ_c value increases, the ratio increases rapidly which means the buckling strength of steel tube with infilled concrete is larger than the hollow tube when λ_c>1.2 and the difference increases as the section slenderness coefficient increases. Another observation from Figure 11 is that the increment is independent from the steel grade and concrete grade.

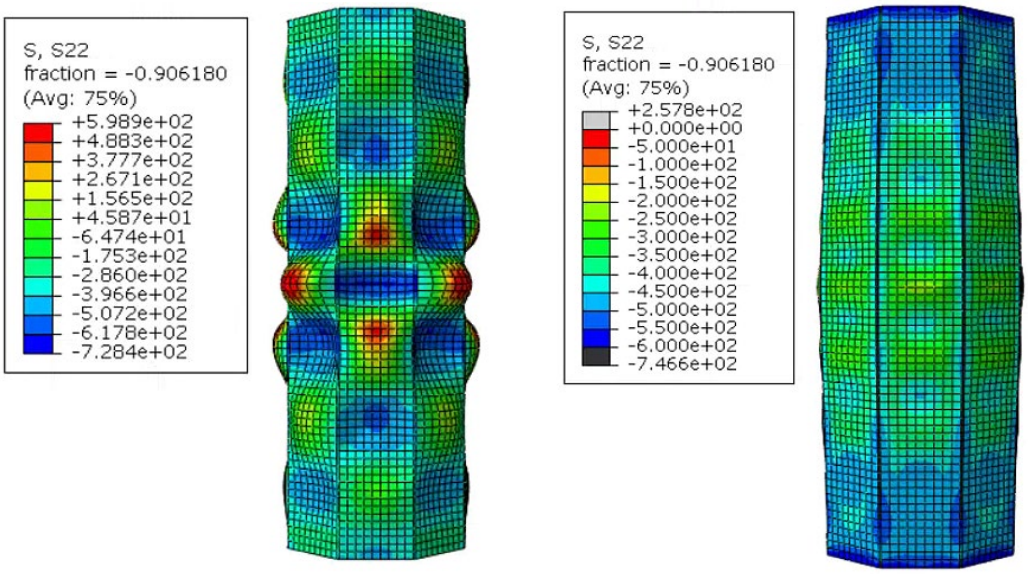

(a) Hollow steel tube (b) CFST

Figure 10. Axial stress distribution nephogram of octagonal steel tube with and without concrete core at peak load

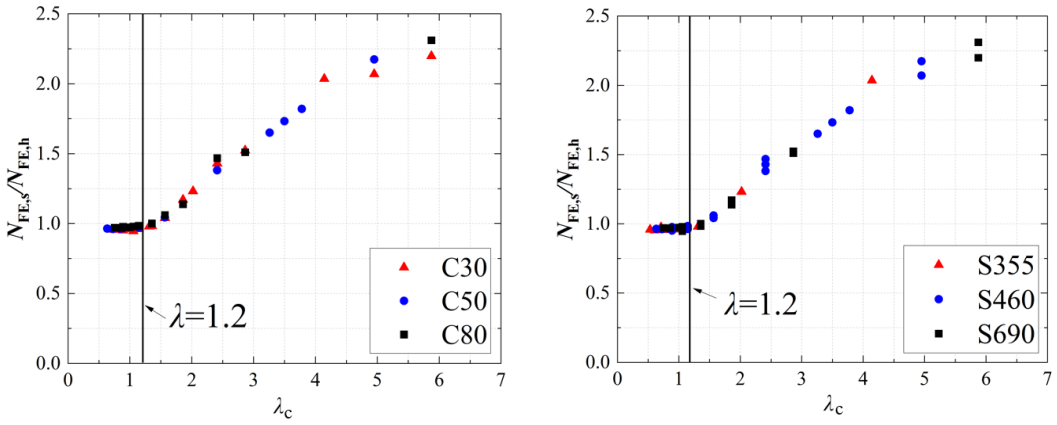

(a) (b)

Figure 11. Reduction factors between steel tube with and without infilled concrete (a) with different concrete strength (b) with different steel grade

2.3.2 Influence of local buckling to the concrete confinement

Effect of confinement is crucial to the load capacity of CFSTs, and the steel tube provides the lateral confining pressure to the concrete core. Thus, to investigate how the local buckling behaviour of steel tube influences the confinement, concrete strength enhancement ratio is defined as follows:

$$CI = N_{CFST,c} / A_c f_c^{'} \tag{14}$$

where $N_{CFST,c}$ is the axial load bearing by concrete core at ultimate condition. It is well known that the effect of confinement is related to the confinement ratio ξ, thus, the influence of section slenderness to the effect of confinement could be investigated by comparing the relationships between concrete strength enhancement and confinement ratio of CFSTs with different section slenderness coefficients. Figure 12 illustrated the relationships between strength enhancement of concrete and confinement ratio of CFSTs with slender and compact section are almost the same. Figure 13 shows the stress-strain curves of concrete from two series of octagonal CFSTs with same confinement ratio. It could be found that the stress-strain relationship of CFST with

different slenderness coefficient are close under the same confinement ratio. In addition, the axial stress distributions of the composite sections with section slenderness coefficient of 2.86 and 0.96 are compared (see Figure 14), it could be found that the axial stress distributions in concrete core with buckled and not buckled steel tubes are similar, this is because the local buckling occurred at the middle portion of the flat sides, where the concrete is not efficiently confined, while in those CFST without local buckling, due to the non-uniform confinement the concrete near the middle portion of the flat sides are not effectively confined either, thus the local buckling has minor impact to the effect of confinement. Based on these observations, it could be concluded that the section slenderness coefficient has minor influence to the confinement effectiveness in octagonal CFSTs.

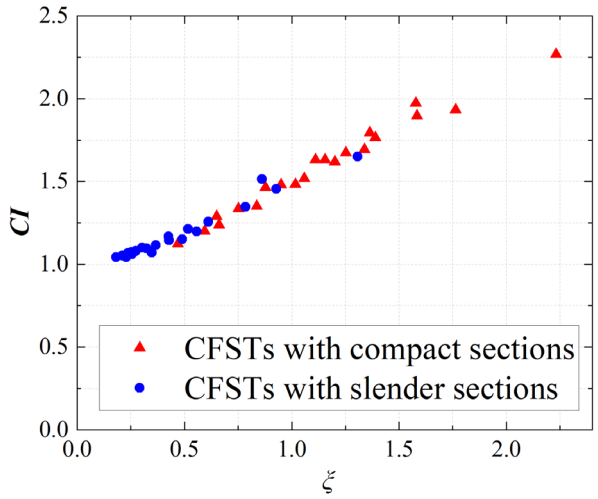

Figure 12. Relationship between strength enhancement of concrete and confinement ratio of CFSTs with slender and compact section

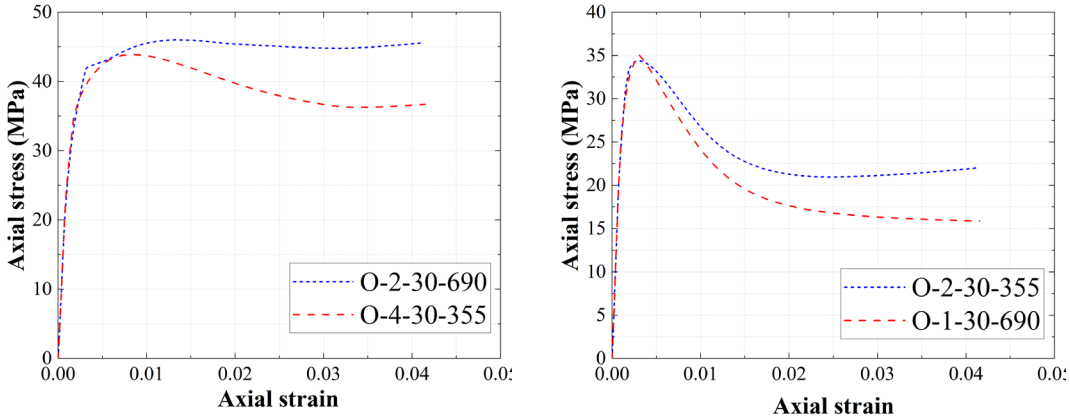

(a) ξ=0.86 (b) ξ=0.42

Figure 13. Comparison of stress-strain curves of infilled concrete with different section slenderness ratio

322

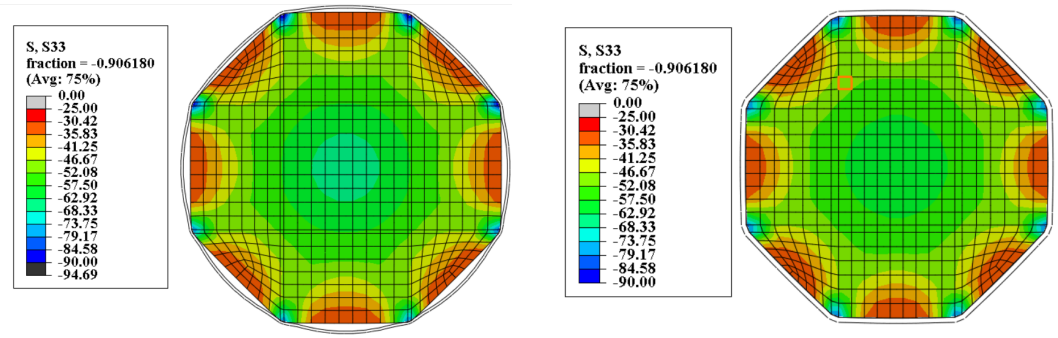

(a) O-2-30-690 (λ_c=2.86) (b) O-4-30-355 (λ_c=0.96)

Figure 14. Comparison of axial stress distribution of infilled concrete with different section slenderness ratio

323

324 3. Design recommendations

325 The design provisions such as Eurocode EN 1994-1-1[14], American standard
326 ANSI/AISC 360-16[15] and Chinese code GB 50936-2014[28] provide the design
327 formulas for the load bearing capacity of CFSTs. Among them, only Chinese code GB
328 50936-2014 covers the octagonal section, while in Eurocode and American standard,
329 only the design formulas of circular and rectangular CFSTs are specified. In all these

standards, limitations of diameter to thickness ratio (*D/t*) for circular section and width to thickness ratio (*b/t*) for rectangular section are recommended to avoid local buckling of steel tube. The limitations of each standards are shown as follows:

$$\text{EN 1994-1-1} \quad \begin{cases} D/t \le 90\dfrac{235}{f_y} & \text{(cirular section)} \\ b/t \le 52\sqrt{\dfrac{235}{f_y}} & \text{(rectagunlar section)} \end{cases} \tag{15}$$

$$\text{ANSI/AISC 360-16} \quad \begin{cases} D/t \le 0.31\dfrac{E}{f_y} & \text{(cirular section)} \\ b/t \le 5.0\sqrt{\dfrac{E}{f_y}} & \text{(rectagunlar section)} \end{cases} \tag{16}$$

$$\text{GB 50936-2014} \quad \begin{cases} D/t \le 135\dfrac{235}{f_y} & \text{(cirular section)} \\ b/t \le 60\sqrt{\dfrac{235}{f_y}} & \text{(rectagunlar section)} \end{cases} \tag{17}$$

As the application of thin-walled tube and high strength steel become popular, the design of CFST with larger *D/t* or *b/t* ratio which exceeds the current limitations may be required. Thus, in following sections, the applicability of current design formulas for the thin-walled octagonal CFST whose section slenderness coefficient exceeds the design limitations was assessed by the experimental and numerical results.

3.1 Existing design formulas and assessment

3.1.1 ANSI/AISC 360-16

American standard ANSI/AISC 360-16 classified the cross section into three categories: compact section, non-compact section and slender section, according to the section slenderness ratio (i.e. *D/t* or *b/t*). For round sections, sections with *D/t* value lower than $\lambda_p = 0.15E/f_y$ are classified as compact section, and those sections with *D/t* value ranges from $0.15E/f_y$ to $0.19E/f_y$ are classified as noncompact section and those

sections with D/t ratio larger than $0.19E/f_y$ but less than the maximum permitted value $0.31E/f_y$ are classified as slender section. Similar classification is also suggested for the rectangular section and the boundaries for compact, noncompact and slender section are $\lambda_p = 2.26(E/f_y)^{1/2}$, $3.0(E/f_y)^{1/2}$ and $5.0(E/f_y)^{1/2}$ respectively. For the compressive strength of noncompact section, ANSI/AISC 360-16 considers the effect of section slenderness and suggests the following equation:

$$N_{\mathrm{AISC}} = N_{\mathrm{p}} - \left(\frac{\lambda_s - \lambda_{\mathrm{p}}}{\lambda_{\mathrm{r}} - \lambda_{\mathrm{p}}} \right)^2 \left(N_{\mathrm{p}} - N_{\mathrm{y}} \right) \tag{18}$$

where λ_s is D/t and b/t values of the circular sections and rectangular sections. N_p is the load capacity of compact section and N_y is given as follows:

$$N_{\mathrm{y}} = A_{\mathrm{s}} f_{\mathrm{y}} + 0.7 A_{\mathrm{c}} f_{\mathrm{c}}^{'} \tag{19}$$

For slender sections, ANSI/AISC 360-16 suggests the following equation to calculate the load capacity of the composite section:

$$N_{\mathrm{y}} = A_{\mathrm{s}} f_{\mathrm{cr}} + 0.7 A_{\mathrm{c}} f_{\mathrm{c}}^{'} \tag{20}$$

where f_{cr} is the buckling stress of the steel section. As the octagonal section is not covered in ANSI/AISC 360-16, two design approaches could be used. One is directly using the equations for rectangular section where the width b is the width of octagonal section and the other one is to use an equivalent diameter for the octagonal section, and in this paper the diameter of inscribed circle of the octagonal section is adopted. Figure 15a shows the comparison of prediction of load capacity from the equations for the rectangular composite section (N_{AISC1}) to the test and FE results (N). It is found that the prediction is very conservative, for those octagonal CFSTs with compact section and non-compact section, the average value of N_{AISC1}/N is about 0.79, and as the slenderness

coefficient increases, the average value of N_{AISC1}/N reduces to 0.65 for those CFSTs with slender section. In Figure 15b, the predictions from the formulas for circular section (N_{AISC2}) are compared with the experimental and numerical results (N) where the inscribed diameter of octagonal section is used. It could be found the formulas for circular section are less conservative, where the average value of N_{AISC2}/N is about 0.82 for compact and noncompact section, and 0.71 for slender section. It should be noted that these two design approaches give difference boundaries for section classification, as shown in Figures 15a and 15b, with the same set of data, more octagonal sections exceed the maximum permitted slenderness coefficient when the equivalent diameter is used.

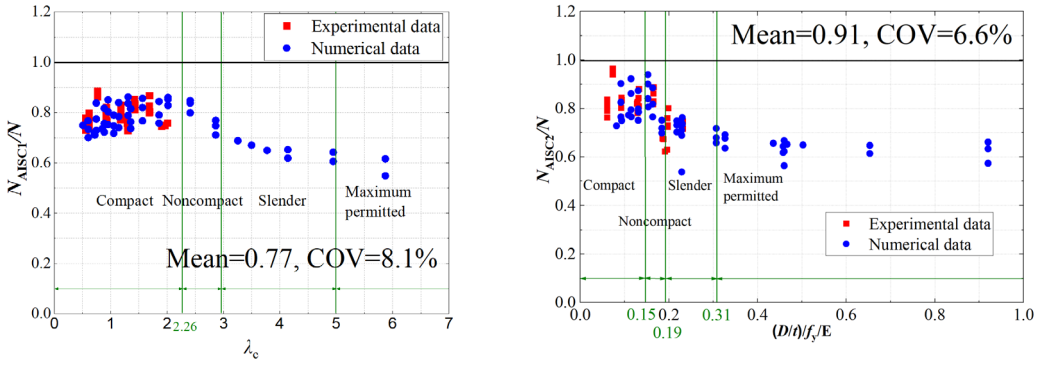

(a) Equations for the rectangular composite section

(b) Equations for the circular composite section

Figure 15. Comparison of load capacity from experimental and numerical results with the predicted capacity from American standard (ANSI/AISC 360-16).

3.1.2 EN 1994-1-1

In Eurocode EN 1994-1-1, two design formulas are suggested for the calculation of load bearing capacity. The first formula is the superposition of the compressive strength of steel and concrete components, the expression is shown as follows:

$$N_{EC4\text{-}1} = A_s f_y + A_c f_c' \tag{21}$$

Another formula is especially for the CFST with circular section which considers the strength enhancement of concrete due to the confinement and the strength reduction of steel tube due to the biaxial stress. The expression is shown as follows:

$$N_{\text{EC4-2}} = \eta_{\text{a}} A_{\text{s}} f_{\text{y}} + \left(1 + \eta_{\text{c}} \frac{t f_{\text{y}}}{D f_{\text{c}}^{'}}\right) A_{\text{c}} f_{\text{c}}^{'} \tag{22}$$

where η_{a} is a reduction factor on the strength of steel, and η_{c} is an enhancement factor to the confined concrete. $\bar{\lambda}$ is the relative slenderness determined by EN 1994-1-1. As the design method in EN 1994-1-1 does not cover the octagonal section, similar design approaches can be used as mentioned in section 4.1.1. Figures 16a and 16b show the comparisons of the predicted capacity from Eq. 22 and Eq. 23 to the test and numerical results respectively. It could be found that Eq. 22 gives conservative predictions with average value of $N_{\text{EC4-1}}/N$ equal to 0.89, and as the section slenderness coefficient increases, the prediction become less conservative. The formula for circular section considers the effect of confinement, and overestimates the strength of octagonal CFSTs with an average $N_{\text{EC4-2}}/N$ value equal to 1.10. Recently, Zhu and Chan[10] proposed a modified design formula based on the Eq. 23 for the octagonal CFSTs. This modified formula uses the inscribed diameter of the octagonal section as an equivalent diameter, and also applies a reduction factor to concrete strength to consider the difference of confinement effectiveness between circular and octagonal section. The modified formula is shown as follows:

$$N_{\text{d}} = \eta_{\text{a,Di}} A_{\text{s}} f_{\text{y}} + \left(1 + 0.73\eta_{\text{c,Di}} \frac{t f_{\text{y}}}{D_i f_{\text{c}}^{'}}\right) A_{\text{c}} f_{\text{c}}^{'} \tag{23}$$

where $\eta_{\text{a,Di}}$ and $\eta_{\text{c,Di}}$ are the reduction and enhancement factors calculated based on the

inscribed diameter. Figure 17 shows the assessment of the Eq. 24 from Zhu and Chan[10]. It could be found this equation provides a good prediction to the load capacity of octagonal CFSTs but the trend shows that for those CFSTs with slender section, the prediction is not conservative as the reduction of strength in steel tube due to the local buckling is not considered.

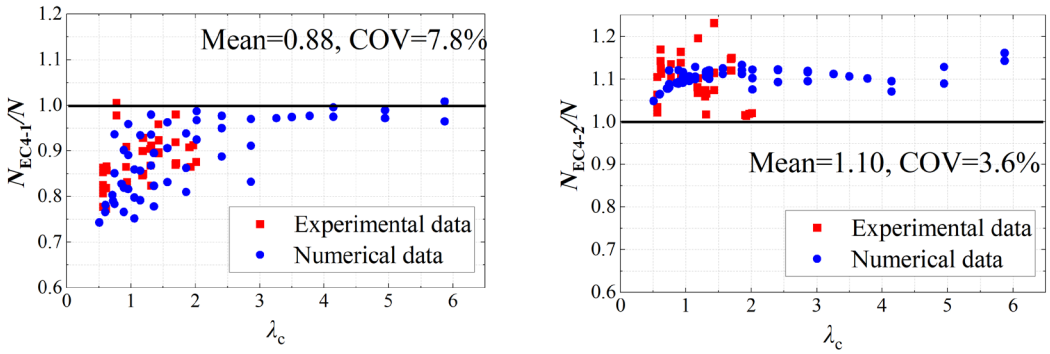

(a) Predictions from Eq. 22 (b) Predictions from Eq. 23

Figure 16. Comparison of load capacity from experimental and numerical results with the predictions from European standard (EN 1994-1-1)

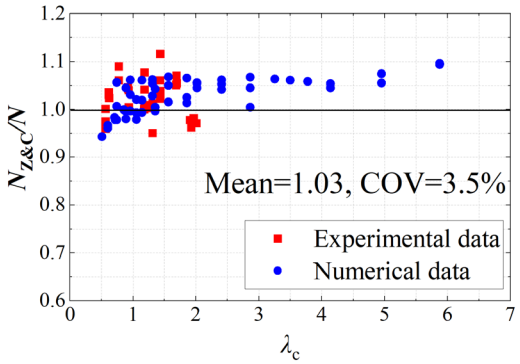

Figure 17. Comparison of load capacity from experimental and numerical results with the predictions from Zhu and Chan[10].

3.1.3 GB 50936-2014

Chinese standard specifies the design formula for CFST with circular, hexadecimal, octagonal and rectangular sections. A cross-sectional strength of composite section is suggested which considers the effect of confinement in concrete core. The expressions are shown as follows:

$$N_{GB} = \left(1.212 + B\theta + C\theta^2\right)\left(A_s + A_c\right) f_{ck} \quad (24)$$

where θ is confinement ratio, B and C are modification factors for different cross-section shapes. f_{ck} is the characteristic compressive strength of concrete. GB 50936-2014 specifies the relationship of the characteristic strength of concrete and the cube strength $f_{cu,k}$ which is from compressive tests on 150 mm × 150 mm × 150 mm cube specimens. The expression is shown as follows:

$$f_{ck} = 0.88\alpha_1\alpha_2 f_{cu,k} \quad (25)$$

where α_1 is the reduction factors that considers the strength difference between cubic test specimens and structural members, and α_2 is the reduction factors accounts for the brittleness of concrete with cube strength larger than 50 MPa. To converge the cube strength to the cylinder strength of concrete, the following relationship was adopted in this paper:

$$f_{cu,k} = 0.8 f_c^{'} \quad (26)$$

Figure 18 shows the comparison of load capacity from experimental and numerical results to the predicted capacity from GB 50936-2014. It could be found that the design formula from GB 50936-2014 gives a very conservative prediction for those compact section (λ_c<1.2), as the section slenderness coefficient increases, the predictions become less conservative as the local buckling behaviour of steel tube is not considered.

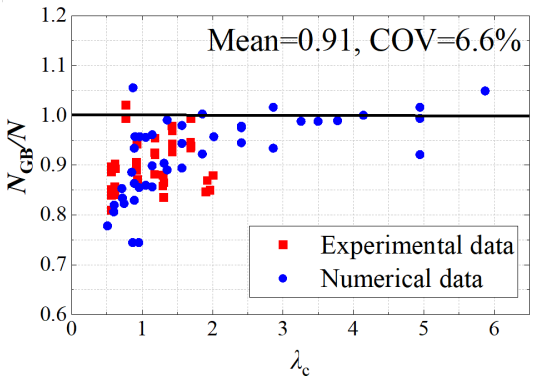

Figure 18. Comparison of load capacity from experimental and numerical results with the predictions from Chinese standard (GB 50936)

3.1.4 Discussion

The assessment has shown that the current design approaches from EN 1994-1-1 are unconservative for the thin-walled octagonal CFST. The predictions can reasonably capture the load capacities of octagonal CFSTs within their specified limit but when the section slenderness exceeds the limit, the design method does not consider the strength reduction in steel tube due to local buckling, which overestimates the capacity contribution from the steel tube. On the contrary, in the American standard (ANSI/AISC 360-16), the strength reduction due to local buckling of the steel tube is over considered, the design formula underestimates the load capacities of the octagonal CFSTs with non-compact and slender section, indicating that the design method for thin-walled rectangular section may not be suitable for octagonal CFSTs. Thus, a new design formula based on the local buckling behavior of octagonal steel tube was proposed.

3.2 Proposed design formula

To accurately capture the strength of the octagonal CFSTs with slender section, the local buckling of steel tube should be considered. The design formula of octagonal hollow section could be used with modification factors to consider the influence of

biaxial stress and infilled concrete core. In this paper, the following equation is established:

$$N_{\text{pro}} = \alpha_s N_{\text{sy}} + \alpha_{\text{c}} N_{\text{c}} \tag{27}$$

where α_{s} is a reduction factor due to the biaxial stress and the local buckling, N_{sy} is the nominal load capacity of steel tube which is equal to $A_{\text{s}}f_{\text{y}}$, α_{c} is the magnified factor due the effect of confinement and N_{c} is the nominal load capacity of concrete core. Based on the relationship of $N_{\text{FE,s}}/N_{\text{sy}}$ and confinement ratio of octagonal CFSTs with compact section ($\lambda_{\text{c}} \leq 1.69$), it was found that the reduction factor α_{s} is equal to a constant 0.95 when the confinement ratio ranges from 0.24 to 1.5. For α_{s} when $\lambda_{\text{c}} > 1.69$, regression analysis was conducted and the expression of α_{s} is obtained as follows (see Figure 19):

$$\alpha_{\text{s}} = \begin{cases} 0.95 & \lambda_{\text{c}} \leq 1.69 \\ 1.08\lambda_{\text{c}}^{-0.2} & \lambda_{\text{c}} > 1.69 \end{cases} \tag{28}$$

For the enhancement factor on concrete core α_{c}, it has been proved that the section slenderness coefficient has minor influence to the confinement index. Thus, α_{c} could be obtained from the relationship between concrete strength enhancement ratio and confinement ratio ξ as shown in Figure 19. The expression is shown as follows:

$$\alpha_{\text{c}} = 0.11\xi^2 + 0.36\xi + 1 \tag{29}$$

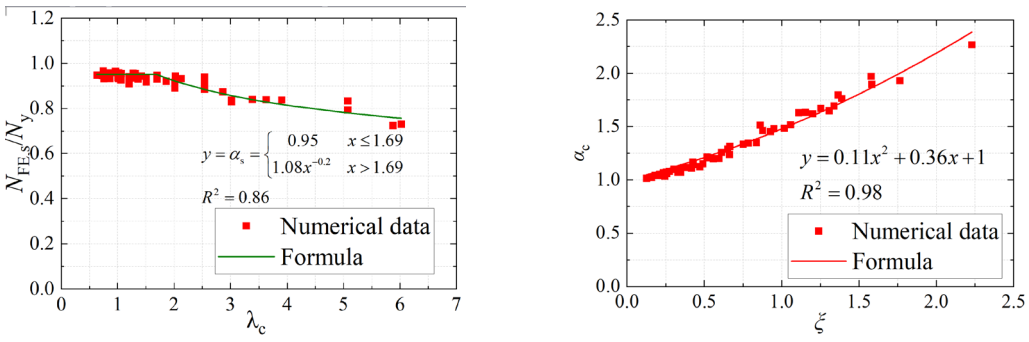

(a) (b)

Figure 19. Proposed expression for (a) α_{s}, (b) α_{c}

Figure 20 shows the predictions of proposed formula to the test and numerical results (N_{pro}/N). A new batch of numerical data of thin-walled octagonal CFSTs (λ_c >1.69) were generated for the assessment. It could be seen that the predictions from the proposed model have good agreements with the test and FE results, the mean value of N_{pro}/N is about 1.00 and COV is 3.7%.

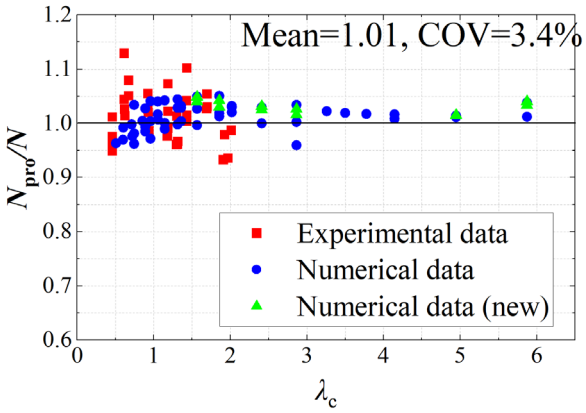

Figure 20. Comparison of load capacity of octagonal CFST between proposed formula and results from database

4. Conclusion

This paper presents a numerical investigation of thin-walled octagonal CFST under uniaxial compression. Finite element analysis was conducted and the models were validated by the collected existing experimental results. Based on the validated model, a parametric study was conducted and a new design model was proposed. The detailed conclusions are summarised as follows:

1. Finite element models for octagonal CFSTs were established and validated by the existing experimental results. The model can well capture both the failure mode and load-shortening curves of octagonal CFSTs.
2. In the parametric study, it was found the infilled concrete can significantly improve

the buckling strength of octagonal steel tubes, the enhancement of the buckling strength increases with the increase of section slenderness coefficient. The buckling behaviour of thin-walled steel tubes has a minor influence on the effect of confinement in the concrete core.

3. The existing code of practices, American standard ANSI/AISC 360-16, Eurocode EN 1994-1-1 and Chinese code GB 50936-2014, were assessed by a database of octagonal CFSTs which includes 37 test specimens and 51 numerical models. It was found that the design methods from EN 1994-1-1 overestimate the load capacity of thin-walled octagonal CFSTs because the strength reduction in steel tube due to local buckling is not considered. However, ANSI/AISC 360-16 who considers the local buckling strength underestimates the load capacity which indicates the current design approaches for thin-walled rectangular section may not suitable for thin-walled octagonal section. GB 50936-2014 is conservative for the octagonal CFSTs with compact section but less conservative for that with slender section.
4. A design model was proposed which is based on the current design method of octagonal hollow steel tubes and considers the effect of infilled concrete core to the buckling strength of slender octagonal steel tubes and the effect of confinement to the concrete core. The model can accurately capture the load-bearing capacity of octagonal CFSTs with compact and slender sections.

Acknowledgement

This work is supported by the National Natural Science Foundation of China (No. 52008238, No. 52208317) and the China Postdoctoral Science Foundation (No.

2020M681266).

Reference:

[1] L.H. Han, Tests on stub columns of concrete-filled RHS sections, Journal of Constructional Steel Research 58(3) (2002) 353-372.
[2] S.P. Schneider, Axially Loaded Concrete-Filled Steel Tubes, Journal of Structural Engineering 124(10) (1998) 1125-1138.
[3] K.A.S. Susantha, H. Ge, T. Usami, Uniaxial stress–strain relationship of concrete confined by various shaped steel tubes, Engineering Structures 23(10) (2001) 1331-1347.
[4] M. Tomii, K. Yoshimura, Y. Morishita, Experimental studies on concrete filled steel tubular stub columns under concentric loading, International Colloquium on Stability of Structures under Static and Dynamic Loads, American Society of Civil Engineers (ASCE), Washington, DC, USA, 1977, pp. 718-741.
[5] J. Chen, T.-M. Chan, Experimental assessment of the flexural behaviour of concrete-filled steel tubular beams with octagonal sections, Engineering Structures 199 (2019) 109604.
[6] J. Chen, T.-M. Chan, R.K.L. Su, J.M. Castro, Experimental assessment of the cyclic behaviour of concrete-filled steel tubular beam-columns with octagonal sections, Engineering Structures 180 (2019) 544-560.
[7] F.-x. Ding, Z. Li, S. Cheng, Z.-w. Yu, Composite action of octagonal concrete-filled steel tubular stub columns under axial loading, Thin-Walled Structures 107 (2016) 453-461.
[8] H. Fang, T.-M. Chan, B. Young, Structural performance of concrete-filled cold-formed high-strength steel octagonal tubular stub columns, Engineering Structures 239 (2021) 112360.
[9] J.-J. Lim, T.-S. Eom, Compression tests of octagonal concrete-filled thin-walled tube columns, Engineering Structures 221 (2020) 111082.
[10] J.-Y. Zhu, T.-M. Chan, Experimental investigation on octagonal concrete filled steel stub columns under uniaxial compression, Journal of Constructional Steel Research 147 (2018) 457-467.
[11] J.-Y. Zhu, T.-M. Chan, Behaviour of polygonal-shaped steel-tube columns filled with high-strength concrete, 171(2) (2018) 96-112.
[12] J. Chen, T.-M. Chan, Compressive behaviour and design of compact to slender octagonal concrete-filled steel tubular stub columns, Thin-Walled Structures 167 (2021) 108211.
[13] M.F. Hassanein, V.I. Patel, M. Elchalakani, H.-T. Thai, Finite element analysis of large diameter high strength octagonal CFST short columns, Thin-Walled Structures 123 (2018) 467-482.
[14] CEN, Eurocode 4: Design of Composite Steel and Concrete Structures Part 1-1: General Rules and Rules for Buildings, EN 1994-1-1, European Committee for Standardization (CEN), Brussels, Belgium, 2004.
[15] ASCE, Specification for Structural Steel Buildings, ANSI/AISC 360-16, American Institute of Steel Construction (AISC), Chicago, IL, USA, 2016.
[16] Q.Q. Liang, B. Uy, J.Y. Richard Liew, Nonlinear analysis of concrete-filled thin-walled steel box columns with local buckling effects, Journal of Constructional Steel Research 62(6) (2006) 581-591.
[17] C.-C. Chen, J.-W. Ko, G.-L. Huang, Y.-M. Chang, Local buckling and concrete confinement of concrete-filled box columns under axial load, Journal of Constructional Steel Research 78 (2012) 8-21.
[18] T. Aoki, Y. Migita, Y. Fukumoto, Local buckling strength of closed polygon folded section columns, Journal of Constructional Steel Research 20(4) (1991) 259-270.

[19] J. Chen, J.-Y. Zhu, T.-M. Chan, Experimental and numerical investigation on stub column behaviour of cold-formed octagonal hollow sections, Engineering Structures 214 (2020) 110669.
[20] H. Fang, T.-M. Chan, B. Young, Behavior of octagonal high-strength steel tubular stub columns, Journal of Structural Engineering 145(12) (2019) 04019150.
[21] A. Godat, F. Legeron, D. Bazonga, Stability investigation of local buckling behavior of tubular polygon columns under concentric compression, Thin-Walled Structures 53 (2012) 131-140.
[22] Y. Migita, Y. Fukumoto, Local buckling behaviour of polygonal sections, Journal of Constructional Steel Research 41(2) (1997) 221-233.
[23] J.-Y. Zhu, T.-M. Chan, B. Young, Cross-sectional capacity of octagonal tubular steel stub columns under uniaxial compression, Engineering Structures 184 (2019) 480-494.
[24] J. Chen, H. Fang, T.-M. Chan, Design of fixed-ended octagonal shaped steel hollow sections in compression, Engineering Structures 228 (2021) 111520.
[25] CEN, Eurocode 3: Design of steel structures – Part 1.1: General rules and rules for buildings, EN 1993-1-1, European Committee for Standardization (CEN), Brussels, 2005.
[26] ASCE, Design of Steel Transmission Pole Structures, ASCE/SEI 48-11, American Society of Civil Engineers (ASCE), Reston, Virginia, 2011.
[27] H. Fang, T.-M. Chan, B. Young, Material properties and residual stresses of octagonal high strength steel hollow sections, Journal of Constructional Steel Research 148 (2018) 479-490.
[28] CABP, Technical Code for Concrete-Filled Steel Tubular Structures, Architecture & Building Press Beijing, China, 2014.
[29] ABAQUS, Dassault Systèmes Simulia Crop. , Johnston, RI, USA, 2022.
[30] J. Chen, H. Liu, T.-M. Chan, Material properties and residual stresses of cold-formed octagonal hollow sections, Journal of Constructional Steel Research 170 (2020) 106078.
[31] Z. Tao, Z.-B. Wang, Q. Yu, Finite element modelling of concrete-filled steel stub columns under axial compression, Journal of Constructional Steel Research 89 (2013) 121-131.
[32] V.K. Papanikolaou, A.J. Kappos, Confinement-sensitive plasticity constitutive model for concrete in triaxial compression, International Journal of Solids and Structures 44(21) (2007) 7021-7048.